

NMR Reciprocity: A Simple(r) Description

Andrew J. Ilott, and Alexej Jerschow*

Department of Chemistry

New York University

New York, NY 10003

* corresponding author: alexej.jerschow@nyu.edu

May 12, 2022

Abstract

In the context of NMR spectroscopy and MRI, the principle of reciprocity provides a convenient method for determining the reception sensitivity from the transmitted rf field pattern. The reciprocity principle for NMR was originally described by Hoult et al. [J. Magn. Reson. (1976),24, 71], and can be seen as being based on the broader Lorentz reciprocity principle, and similar theorems from antenna theory. One particular implication of the reciprocity principle is that if a single coil is used for both transmission and detection, the two fields can be assumed to be equal. This aspect is also where some of the conceptual difficulty of applying the theorem may be encountered. For example, the questions of whether one should use the complex conjugate field for detection, or whether one should apply the theorem in the rotating frame or the laboratory frame are often where considerable confusion may arise, and incorrect results may be derived. We attempt here to provide a simple discussion of the application of the reciprocity principle in such a way as to clarify some of the confounding questions. In particular, we avoid the use of the ‘negatively rotating frame’, which is frequently mentioned in this context, since we consider it to unnecessarily complicate the matter. In addition, we also discuss the implications of the theorem for magnetic resonance experiments on conducting samples, and metals, in particular.

1 Introduction

The principle of reciprocity for magnetic resonance [6, 7] has been used to determine coil sensitivities and the spatial distributions of the detected signals. In the description provided below, we lean heavily on concepts discussed in Refs [1, 4, 13], but provide a somewhat different account of the matter in an attempt to simplify the discussion and provide a straightforward conceptual picture of the effects in question. As mentioned by Hoult [4], complex numbers are often used in two different ways in the description of the fields, from which inconsistencies can arise. One of their uses is to indicate the positively and negatively rotating frames [4]. We avoid the discussion of the different rotating frames, as we believe such a construct is more of an impediment than help in properly applying the reciprocity principle.

One particularly illustrative demonstration of the reciprocity principle consists of describing an experiment wherein one uses two coils, with one being driven by an ac or rf field and the other one connected to a detector/oscilloscope [4]. The voltage induced in one coil by driving the other with unit current is the same whichever coil is chosen for each role. This outcome is found irrespective of the shapes and the geometrical arrangements of the two coils. By extension, it was argued, one could think of the effect of the driving coil as being represented by a magnetic dipole, or a magnetization \mathbf{M} corresponding to the induced field that would be created by the current passed through the coil (see Fig. 1). For example, for a small circular loop, the strength of the dipole would be given by $\mu = Ia$, where I is the current, and a is the area of the loop. For irregular shapes, the use of the magnetization \mathbf{M} , would be a more suitable approach, since \mathbf{M} describes the spatially varying dipole density and thus provides a more general description. One could thus think of an irregularly-shaped coil, which, when a current passes through it, is modeled by a spatially varying \mathbf{M} distribution. A particularly visual illustration of these points is made in Fig. 2 of Ref [5].

The induced emf ξ induced in the receiving coil is given by

$$\xi = d\Phi/dt, \tag{1}$$

where Φ is the flux through the coil determined by

$$\Phi = \int_A \mathbf{B}^M \cdot d\mathbf{a}, \tag{2}$$

with \mathbf{B}^M being the field produced by the magnetization. The integral runs over the receiving coil area.

The NMR reciprocity expression is given as

$$\xi = -\frac{d}{dt} \int_V \mathbf{B}_1(\mathbf{r}) \cdot \mathbf{M}(\mathbf{r}, t) d^3r, \tag{3}$$

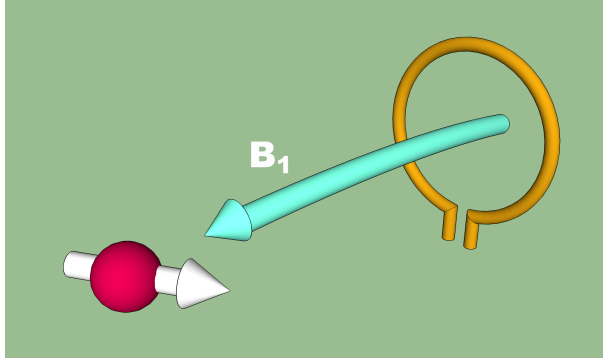


Figure 1: A spin in the presence of an rf-field generated by a coil. The reciprocity principle provides a relationship between the transmitted and the detected fields.

where V is the sample volume, \mathbf{M} is the sample magnetization, and \mathbf{B}_1 is the rf field generated by the receive coil at the position of the magnetization if a unit current were passed through it [4, 5]. A derivation of this expression is given in the Appendix. In this article, we will refer to both \mathbf{H} and \mathbf{B} magnetic fields, because this is how they are often referred to in the magnetic resonance literature, although it is recognized that in many texts the term ‘magnetic induction’ or ‘magnetic flux density’ would be used for \mathbf{B} .

Eq. (3) is to be interpreted as follows: a unit magnetization at position \mathbf{r} will induce an emf in the receiving coil that is proportional to the magnetic field \mathbf{B}_1 that would be generated by the coil at position \mathbf{r} if a unit current were passed through the coil. The most useful aspect of this expression for NMR purposes is obtained when one uses for \mathbf{M} the magnetization obtained as a result of the application of the rf field, which is further discussed below.

Expanding the scalar product and neglecting the z -component in the scalar product (because the time derivative of that product would be negligible, i.e. the change in M_z is slow compared to precession motion), one obtains

$$\xi = -\frac{d}{dt} \int_V [B_{1x}(\mathbf{r})M_{1x}(\mathbf{r}, t) + B_{1y}(\mathbf{r})M_{1y}(\mathbf{r}, t)] d^3r, \quad (4)$$

If the apparatus were rotated, we would not expect a change of the measured quantities. It is therefore useful to convert to a notation of amplitude and phase in both components. The most straightforward way for this transition is provided by a complex-valued notation (similar to the treatment in [1]), wherein the orientation-dependent factor will be easy to separate out. In complex notation, we have

$$\xi = -\frac{d}{dt} \int_V B_{1+}(\mathbf{r})M_-(\mathbf{r}, t) d^3r, \quad (5)$$

where

$$B_{1\pm} = B_{1x} \pm iB_{1y} \quad (6)$$

$$M_{\pm} = M_x \pm iM_y, \quad (7)$$

and using the amplitudes and phases for both quantities according to

$$B_{1+} = B_{1\perp} \exp(i\phi_r) \quad (8)$$

$$M_- = M_{\perp} \exp(-i\phi_M) \quad (9)$$

for a counter-clockwise rotation by the respective angles in the $x - y$ plane. We call ϕ_r the receive phase, and ϕ_M will be the magnetization phase, which ultimately will be related to the transmit phase ϕ_t , because the magnetization would be excited by a transmit field with some phase. All these phases depend on the coordinate \mathbf{r} .

After these adjustments, we have

$$\xi = -\frac{d}{dt} \int_V B_{1\perp}(\mathbf{r}) M_{\perp}(\mathbf{r}, t) \exp(i\phi_r - i\phi_M) d^3r. \quad (10)$$

If both the coil and the spins were physically rotated by the same angle (by rotating the whole apparatus, for example), i.e. $\phi_r = \phi_M$, no global phase factor would arise [4].

In the general case, however, say if the coil and the spins were rotated by different amounts, a complex-valued emf ξ would be obtained from this expression. Although the induced emf should be real-valued, one can interpret and construct a complex-valued emf by combining two measurements after signal mixing in two channels which are 90° out of phase from each other. Combining these signals as real and imaginary parts produces the complex-valued measurement of the emf (see, for example [1]). Of course, this procedure can only work when the signal is modulated, which would be the case for precessing magnetization, as discussed below. Any non-canceled initial phase difference between the field and the magnetization will therefore appear as a rotation in the complex plane of the recorded complex signal.

Both physical rotation and time delay in the transmit field can produce a phase, and hence one can compensate one with the other, which is the strategy employed with quadrature coils (see below), or in general when circularly-polarized fields are generated.

2 Detected emf after applying a pulse

For the moment we are going to leave aside the effects of a global rotation of the coil and the magnetization, and any signal delays, so that $\phi_r = 0$. We now examine the measured emf after applying a pulse.

We consider that the transverse magnetization is created by the application of an rf field with amplitude $2B_{1\perp}(\mathbf{r}) \cos(\omega_0 t)$, with ω_0 being the resonance frequency of the nucleus

in question. We include a factor 2 here for convenience. Decomposing this field into a co-rotating and counter-rotating field (with respect to the spin's rotating frame), one obtains

$$2B_{1\perp}(\mathbf{r}) \cos(\omega_0 t) = B_{1\perp}(\mathbf{r}) [\exp(-i\omega_0 t) + \exp(i\omega_0 t)]. \quad (11)$$

The $\exp(-i\omega_0 t)$ component will be co-rotating with the precessing spins and will be the component that leads to pulse excitation. The counter-rotating field produces negligible effects, since the field rotates at twice the Larmor frequency with respect to the precessing spins. Applying this field for a duration τ , flips the magnetization by an angle $\alpha = \gamma|B_{1\perp}(\mathbf{r})|\tau$, and one obtains according to the Bloch equations,

$$M(\mathbf{r}, t) = -iM_0(\mathbf{r}) \sin(\alpha) \frac{B_{1\perp}(\mathbf{r})}{|B_{1\perp}(\mathbf{r})|} \exp(-i\omega_0 t), \quad (12)$$

where M_0 is the equilibrium magnetization. The incurred phase of $-i$ indicates that the magnetization lags the excitation field by 90° . In the context of Eq. (10), this would indicate that $\phi_M = \phi_r + \pi/2$ and

$$M_{\perp}(\mathbf{r}, t) = M_0(\mathbf{r}) \sin(\alpha) \frac{B_{1\perp}(\mathbf{r})}{|B_{1\perp}(\mathbf{r})|} \exp(-i\omega_0 t). \quad (13)$$

Inserting these expressions for M_{\perp} into Eq. (10) gives

$$\xi = i \frac{d}{dt} \int_V \left[M_0(\mathbf{r}) \sin(\alpha) \frac{(B_{1\perp}(\mathbf{r}))^2}{|B_{1\perp}(\mathbf{r})|} \exp(-i\omega_0 t) \right] d^3r. \quad (14)$$

Next, one can take the time-derivative and obtain

$$\xi = \omega_0 \int_V \left[M_0(\mathbf{r}) \sin(\alpha) \frac{(B_{1\perp}(\mathbf{r}))^2}{|B_{1\perp}(\mathbf{r})|} \exp(-i\omega_0 t) \right] d^3r. \quad (15)$$

Taking a Fourier Transform of this time-signal, we then obtain

$$\xi(\omega) = (2\pi)^3 \omega_0 \delta(\omega - \omega_0) \int_V \left[M_0(\mathbf{r}) \sin(\alpha) \frac{(B_{1\perp}(\mathbf{r}))^2}{|B_{1\perp}(\mathbf{r})|} \right] d^3r. \quad (16)$$

with $\delta(\omega - \omega_0)$ being the Dirac delta-function, and the factor $(2\pi)^3$ arising from the Fourier Transform.

It is now important to consider that the quantity $B_{1\perp}$ can itself be complex, where the phase would indicate an advance or lag of the field with respect to the rotating frame. It is clear that if the sample induced a phase in $B_{1\perp}$, this phase would be doubled in the observed signal according to Eq. (16)! This effect is also in line with Eq. (28) of Ref. [4]. We examine this situation in more detail in a couple of examples below.

3 Propagating waves

A simple example of the application of Eq. (16) would be the analysis of an experiment with an rf field propagating through the sample volume along coordinate x , in which case it could be expressed as $B_{1\perp} = B_{1\perp}^0 \exp(-ikx)$, with the wave-vector $k = \omega_0/v$, where $v = 1/\sqrt{\epsilon\mu}$ being the speed of the wave in the medium (phase velocity).

In this case, using expression (16) would produce

$$\xi(\omega) = (2\pi)^3 \omega_0 \delta(\omega - \omega_0) \int_V \left[M_0(\mathbf{r}) \sin(\alpha) \frac{(B_{1\perp}^0(\mathbf{r}))^2}{|B_{1\perp}(\mathbf{r})|} \exp(-2ikx) \right] d^3r, \quad (17)$$

and the phase originally contained in $B_{1\perp}$ is doubled as noted before! This is in stark contrast with the phase originating from a global rotation, which cancels out. As has been mentioned by Hoult [4], an intuitive picture of this phenomenon could also be drawn by examining the situation of an rf field propagating through a coaxial cable: in this case it is perfectly acceptable that the incurred phase in the measured signal has to double, because the rf has to propagate along the cable, and the detected signal has to propagate the same way backwards. This property of uncanceled phases lies at the heart of the ability to detect material-induced phases, and is used in electric property tomography (EPT) [12], for example, but is also important for the investigation of signals originating from conductors, as will be discussed below. A more general description of such processes can be obtained using retarded potentials [10, 14]. Specifically, it is found that the reciprocity expression of Eq. (3) still holds, if the retarded B'_1 field is used [10],

$$\mathbf{B}'_1 = \frac{\mu_0}{4\pi} \int e^{ikr} (1 - ikr) \frac{d\mathbf{l} \times \mathbf{r}}{r^3} \quad (18)$$

4 Using different coils for excitation and detection

Following the same procedure as above, but keeping the transmit ($B_{1\perp}^t$) and the receive fields ($B_{1\perp}^r$) separate, one obtains

$$\xi(\omega) = i(2\pi)^3 \omega_0 \delta(\omega - \omega_0) \int_V \left[M_0(\mathbf{r}) \sin(\alpha) \frac{B_{1\perp}^r(\mathbf{r}) B_{1\perp}^t(\mathbf{r})}{|B_{1\perp}^t(\mathbf{r})|} \exp(i\phi_r - i\phi_t) \right] d^3r. \quad (19)$$

where ϕ_r is the receive phase and ϕ_t the transmit phase related to geometrical rotation only (Fig. 2). Any propagation-related phases (due to delays) would be contained within $B_{1\perp}^t$ and $B_{1\perp}^r$, and would add with the same sign. Here again, note that no complex conjugation is used in the multiplication of the fields, which would lead to incorrect and unphysical results (e.g. time-delays would not add up).

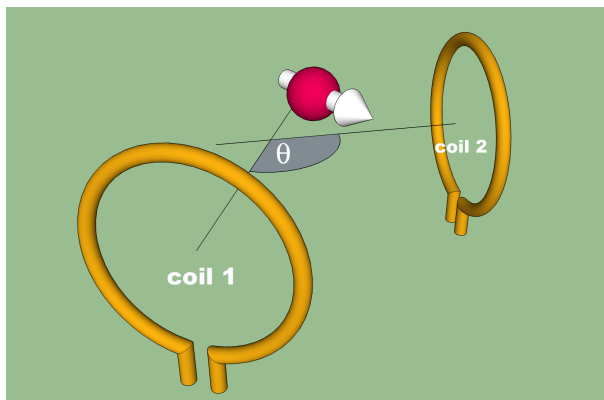


Figure 2: Two-coil arrangement and quadrature excitation / detection. The transmit phases of the two coils would be related by $\phi_{t,1} = \phi_{t,2} + \theta$

5 Quadrature coils, circular polarization

Quadrature coils are often employed by placing two coils at an angle of $\pi/2$ with respect to each other. The transmit phases for the coils in the ideal case are $\phi_{1,t} = 0$, and $\phi_{2,t} = \pi/2$. In order for the B_1 fields originating from the two coils to be aligned with each other at all times, they can be supplied with time-shifted rf fields such that these (geometrical) phases are compensated exactly. So, for example, if the rf-field supplied to the second coil is delayed in phase by $\pi/2$ (e.g. by a quadrature hybrid), the overall geometric phase difference between the coils is canceled and the field vectors from both coils align with each other at all times in the rotating frame of the spins.

Because the receive phase ϕ_r in Eq. (10) enters the equation with the opposite sign, in receive mode, the situation is exactly reversed, and to make sure the signal combines constructively in detection mode, the signal induced in the second coil now has to be advanced in phase by $\pi/2$ relative to the signal of the first coil before combining them. Therefore, for the recorded signal, the overall phase difference between the signals acquired from each coil would be eliminated.

It is clear that this constructive interference in both the transmit and receive mode will not work perfectly over the whole volume but will only be observed in those locations where the geometrical relationship between the two fields is matched by the phase advance (or lag) in the signals supplied to (or received from) the coils.

Along the same lines, one can analyze a birdcage coil or phased arrays that are supplied with appropriately phase-shifted fields such that the fields they produce combine constructively in the region of interest. In these situations, it is customary to speak of the transmit B_{1+} field and the receive B_{1-} field, although it should be emphasized that B_{1+} and B_{1-} here refer simply to the way in which the supplied signals are time-shifted with respect to

each other in order to compensate for geometry-induced phases. This is a point of much confusion, stoked by the use of multiple conventions and notions of the ‘counter-rotating frame’, because it creates the impression that one should use these quantities directly in Eq. (5). This approach would lead to incorrect results.

For example, in electric property tomography [12], it is often suggested that one needs to have a good representation of both the transmit B_{1+} and the receive B_{1-} field. While one has direct access to the magnitude of B_{1+} by standard rf field mapping methods, it is unclear how one should estimate B_{1-} . Often, the approximation $B_{1+} \approx B_{1-}^*$ is used for lack of direct measures of B_{1-} . For example, when attempting to transmit with a B_{1-} polarization, one would enable constructive interference of a rotating field that is opposite to the precession motion of the spins. Therefore, there would be no significant excitation (except for the areas of the sample volume where there are non-ideal phase relationships). By the same token, using a quadrature coil operating in detection mode with B_{1+} polarization would again rotate in the wrong direction, and thus any available signals would interfere destructively upon combination of the channels.

This problem and ambiguity is rooted in practical and fundamental limitations. If the phase compensation were working perfectly for all locations of interest, there would be no overall transmit or receive phase. One limitation arises from misalignment, spatial distribution of field directions, and the fact that quadrature coils cannot be completely isolated, and a more serious problem arises from the influence of the sample on the fields. Specifically, a significant conductivity in the sample will produce an imbalance between the B_{1-} and B_{1+} fields [17]. Since electrical property tomography aims to measure distributions of conductivities in samples, the very property that one desires to measure produces distortions that complicate such measurements with this imbalance.

Note, that it may seem that there should be no difference in B_{1-} and B_{1+} fields if a single coil were driven with linear polarization. A sample displaying a significant amount of conductivity would again produce an imbalance between those two fields. On the other hand, while the amplitude of B_{1+} may vary asymmetrically across the sample, the B_{1+} phase of the signal, needed for EPT, can still be calculated by taking half of the recorded signal phase. The measurement of the B_{1-} field is not required in this case. Linear polarization, of course, always comes at the price of poorer sensitivity, and often also poorer homogeneity.

6 Detecting a signal from a conducting region

We now examine the case where the rf field enters a conductive region, and specifically focus on the situation of a good conductor for the purposes of illustrating the phase doubling effect. In such a case, one obtains the expression for the rf field from the Maxwell equations,

$$\nabla^2 \mathbf{B} = \mu\epsilon \frac{\partial^2 \mathbf{B}}{\partial t^2} + \mu\sigma \frac{\partial \mathbf{B}}{\partial t}. \quad (20)$$

The solution to these equations leads to the plane-wave expression [3, 11]

$$B(\mathbf{r}) = B_{10} e^{-\kappa_- \hat{\mathbf{n}} \cdot \mathbf{r}} e^{i\kappa_+ \hat{\mathbf{n}} \cdot \mathbf{r} - i\omega t}, \quad (21)$$

with B_{10} the rf field at the surface of the conductor, $\hat{\mathbf{n}}$, a unit vector, denoting the propagation direction, \mathbf{r} the location vector, and κ_+ and κ_- the real and imaginary parts of the wave vector, $\kappa = \kappa_+ + i\kappa_-$, defined by [11],

$$\kappa_{\pm} = \sqrt{\mu\varepsilon} \frac{\omega}{c} \left[\frac{1}{2} \sqrt{1 + \left(\frac{2\sigma}{\nu\varepsilon} \right)^2} \pm \frac{1}{2} \right]^{\frac{1}{2}}. \quad (22)$$

Here, ε is the dielectric constant of the conductor and c the speed of light in a vacuum. For a good conductor $\left(\frac{2\sigma}{\nu\varepsilon}\right) \gg 1$ and $\kappa_+ \approx \kappa_- \approx 1/\delta$ (the inverse of the skin depth constant defined in Eq. 23), resulting in the same depth-dependence for both the phase and amplitude of the wave. The skin-depth is given as

$$\delta = \sqrt{\frac{1}{\pi\mu\nu\sigma}}, \quad (23)$$

where ν is the frequency of the field, μ the permeability of the conductor and σ its conductivity. As an example, for lithium metal, $\sigma = 1.08 \times 10^7 \text{ S m}^{-1}$ and $\varepsilon \approx \varepsilon_0 = 8.85 \times 10^{-12} \text{ F m}^{-1}$ at radio frequencies, defining Li as a good conductor in the frequency regime $\nu \ll 2.44 \times 10^{18} \text{ Hz}$, and thus well beyond the radio-frequency and microwave regions.

When incident on a well conducting surface, assuming that the surface extends to infinity, the boundary conditions dictate that only the rf field parallel to the surface remains, and the field within the conductor in the rotating frame can be described by

$$\tilde{B}_1(r) = B_{10} e^{-r/\delta} e^{ir/\delta}, \quad (24)$$

where r denotes the penetration distance from the surface. The rf field decays exponentially and is also acquires a phase shift linear in the propagation depth, as illustrated in Fig. 3.

The flip angle imparted on the spin magnetization by this field is given by

$$\alpha(r) = \gamma\tau |B_{10}| e^{-\beta r} = \alpha(0) e^{-\beta r}, \quad (25)$$

where $\alpha(0)$ is the flip angle at the surface of the conductor.

Using this field in Eq. (10), the voltage induced in the detection coil is given by the integral of the contributions from each depth,

$$\xi = -i(2\pi)^3 \omega_0 \delta(\omega - \omega_0) M_0 \frac{B_{10}^2}{|B_{10}|} \int_{r=0}^{\infty} e^{2ir/\delta} e^{-r/\delta} \sin[\alpha(r)] dr. \quad (26)$$

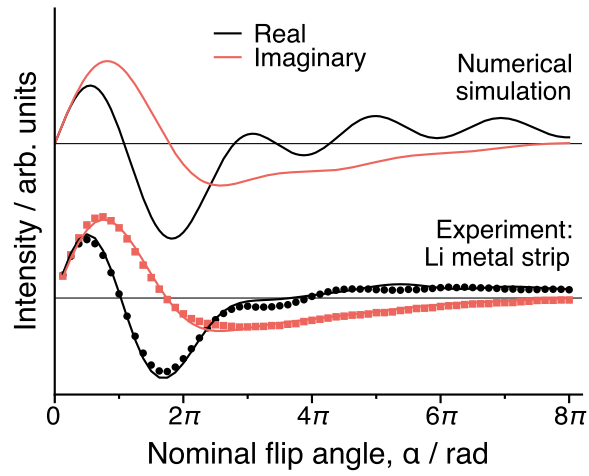
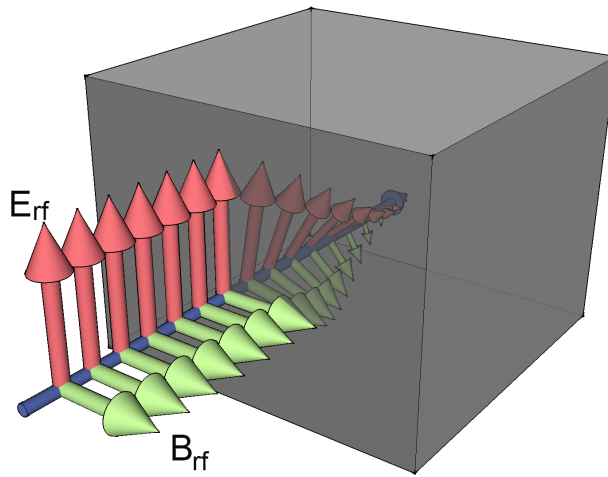


Figure 3: Top: illustration of rf propagation into a conductive region; Bottom: nutation curves, simulation and experiment.

The phase term $e^{2ir/\delta}$ illustrates the aforementioned phase-doubling effect, and governs the extent of constructive or destructive interference between the signals from different depths. An expression equivalent to Eq. (26) was earlier derived by Mehring et al. [15] and used in NMR/MRI of electrochemical cells and with conducting samples [2, 8, 9].

A sensitive verification of Eq. (26) can be produced by a nutation experiment in which the MR signal is measured as a function of the flip angle, α , which is varied experimentally by changing the B pulse duration, τ . An experimental ${}^7\text{Li}$ NMR nutation curve performed on a rectangular piece of natural abundance lithium metal (thickness $\gg \delta$) is shown in Fig. 3 along with a numerical simulation of Eq. (26).

The nutation curve for lithium metal was obtained on a Bruker Ultrashield 9.4 T Avance I spectrometer operating at 155.5 MHz for ${}^7\text{Li}$, using a Bruker ${}^1\text{H}/{}^7\text{Li}$ WB40 birdcage coil for acquisition. The nominal flip angle was calibrated to LiCl(aq) ($\tau_{\pi/2} = 38 \mu\text{s}$). The sample consisted of a strip of natural abundance lithium metal (Aldrich 99.9%) cut to ca. 0.4 x 8 x 15 mm and sealed inside a 10 mm NMR tube. Spectra were acquired on resonance with the center of the metal peak and the plotted intensity profiles correspond to the on-resonance position in the spectrum.

There is excellent agreement between the experimental curve and the calculated one, particularly at lower flip angles $< 3\pi$. Bloch equation simulations including relaxation during the pulse and rf inhomogeneity (20% variation in B_{10} [8]) account for the differences for $\alpha > 3\pi$ and produce a good fit with the experimental results.

7 Conclusions

We have attempted to provide here a concise summary of the issues encountered in discussions of NMR reciprocity. We specifically avoid the discussion of the negatively rotating frame, which we believe is the source of some confusion, and attempt to delineate other related topics, such as quadrature detection. One particular example, which provides a good experimental illustration of the effect of ‘phase doubling’ is shown here as well, the case of signals excited and obtain from within a conductive sample region. It is hoped that this article could contribute to clarifications of different aspects of the use of the NMR reciprocity principle.

Appendix

Derivation of reciprocity principle

We show here one particular derivation of the reciprocity principle. This one is based on Ref. [13].

The fields used in the expressions below will be the time-harmonic fields, given by the

definitions

$$\mathbf{H}_{\text{lab}} = \text{Re} \{ \mathbf{H}(\mathbf{r}) \exp(i\omega t) \} \quad (27)$$

$$\mathbf{B}_{\text{lab}} = \text{Re} \{ \mathbf{B}(\mathbf{r}) \exp(i\omega t) \} \quad (28)$$

$$\mathbf{M}_{\text{lab}} = \text{Re} \{ \mathbf{M}(\mathbf{r}) \exp(i\omega t) \} \quad (29)$$

$$\mathbf{E}_{\text{lab}} = \text{Re} \{ \mathbf{E}(\mathbf{r}) \exp(i\omega t) \}. \quad (30)$$

The fields generated by the magnetization \mathbf{M} will be labeled \mathbf{H}^{M} , and \mathbf{E}^{M} , and the expression $\kappa = \sigma + i\omega\epsilon$ will be used. With these definitions, we have for the relevant Maxwell Equations in the space without magnetization

$$\nabla \times \mathbf{E} = -i\omega\mu_0\mathbf{H} \quad (31)$$

$$\nabla \times \mathbf{H} = \kappa\mathbf{E}, \quad (32)$$

and

$$\nabla \times \mathbf{E}^{\text{M}} = -i\omega\mu_0(\mathbf{H}^{\text{M}} + \mathbf{M}) \quad (33)$$

$$\nabla \times \mathbf{H}^{\text{M}} = \kappa\mathbf{E}^{\text{M}}, \quad (34)$$

in the space where magnetization is present, and

$$\nabla \times \mathbf{H} = \kappa\mathbf{E} + \mathbf{J}_c, \quad (35)$$

in a region without magnetization, but with filamentary current flow \mathbf{J}_c .

The induced emf (also time-harmonic here) is given as follows:

$$\xi = \oint \mathbf{E}^{\text{M}} \cdot d\mathbf{l}_r = \int \frac{1}{I} \mathbf{E}^{\text{M}} \cdot \mathbf{J}_c d\mathbf{r} \quad (36)$$

$$= \frac{1}{I} \int \mathbf{E}^{\text{M}} \cdot (\nabla \times \mathbf{H} - \kappa\mathbf{E}) d\mathbf{r} \quad (37)$$

$$= \frac{1}{I} \int \left[\mathbf{E}^{\text{M}} \cdot \nabla \times \mathbf{H} - \underbrace{\nabla \times \mathbf{H}^{\text{M}} \cdot \mathbf{E}}_{\kappa\mathbf{E}^{\text{M}}} \right] d\mathbf{r} \quad (38)$$

$$= \frac{1}{I} \int \underbrace{\nabla \cdot (\mathbf{E}^{\text{M}} \times \mathbf{H} - \mathbf{E} \times \mathbf{H}^{\text{M}})}_{=0} d\mathbf{r} \quad (39)$$

$$- \frac{1}{I} \int [\nabla \times \mathbf{E}^{\text{M}} \cdot \mathbf{H} - \nabla \times \mathbf{E} \cdot \mathbf{H}^{\text{M}}] d\mathbf{r} \quad (40)$$

$$= \frac{1}{I} \int \left[\underbrace{i\omega\mu_0(\mathbf{H}^{\text{M}} + \mathbf{M}) \cdot \mathbf{H}}_{-\nabla \times \mathbf{E}^{\text{M}}} - \underbrace{i\omega_0\mu_0\mathbf{H} \cdot \mathbf{H}^{\text{M}}}_{\nabla \times \mathbf{E}} \right] d\mathbf{r} \quad (41)$$

$$= \frac{1}{I} i\omega_0\mu_0 \int \mathbf{M} \cdot \mathbf{H} d\mathbf{r}, \quad (42)$$

Other recommended derivations include one by Haacke [1], by Hoult [4], by James Tropp [16], and by van der Klink [18].

Acknowledgements

The authors acknowledge funding from the US National Science Foundation under award CHE-1710046.

References

- [1] R. W. Brown, E. M. Haacke, Y.-C. N. Cheng, M. R. Thompson, and R. Venkatesan. *Magnetic resonance imaging: physical principles and sequence design*. John Wiley & Sons, 2014.
- [2] S. Chandrashekar, N. M. Trease, H. J. Chang, L.-S. Du, C. P. Grey, and A. Jerschow. 7Li MRI of Li batteries reveals location of microstructural lithium. *Nat. Mat.*, 11(4):311, 2012.
- [3] D. J. Griffiths. *Introduction to electrodynamics*. Prentice Hall, 1962.
- [4] D. Hoult. The principle of reciprocity in signal strength calculations: a mathematical guide. *Concepts Magn. Reson. A*, 12(4):173–187, 2000.
- [5] D. Hoult. The principle of reciprocity. *J. Magn. Reson.*, 213(2):344–346, 2011.
- [6] D. Hoult and R. Richards. The signal-to-noise ratio of the nuclear magnetic resonance experiment. *J. Magn. Reson.*, 24(1):71–85, 1976.
- [7] D. I. Hoult and R. Richards. The signal-to-noise ratio of the nuclear magnetic resonance experiment. *J. Magn. Reson.*, 213(2):329–343, 2011.
- [8] A. J. Ilott, S. Chandrashekar, A. Kloeckner, H. J. Chang, N. M. Trease, C. P. Grey, L. Greengard, and A. Jerschow. Visualizing skin effects in conductors with mri: 7Li MRI experiments and calculations. *J. Magn. Reson.*, 245:143–149, 2014.
- [9] A. J. Ilott and A. Jerschow. Super-resolution surface microscopy of conductors using magnetic resonance. *Sci. Rep.*, 7(1):5425, 2017.
- [10] E. Insko, M. Elliott, J. Schotland, and J. Leigh. Generalized reciprocity. *J. Magn. Reson.*, 131(1):111 – 117, 1998.
- [11] J. D. Jackson. *Classical electrodynamics* john wiley & sons. *Inc., New York,*, 1999.

- [12] U. Katscher, T. Voigt, C. Findekklee, P. Vernickel, K. Nehrke, and O. Doessel. Determination of electric conductivity and local sar via b1 mapping. *IEEE Trans Med Imag*, 28(9):1365–1374, 2009.
- [13] S. J. Keun, W. E. Je, and K. Ulrich. *Electro-magnetic tissue properties MRI*, volume 1. World Scientific, 2014.
- [14] C. Mahony, L. Forbes, S. Crozier, and D. Doddrell. A novel approach to the calculation of RF magnetic and electric fields for NMR coils of arbitrary geometry. *J. Magn. Reson., Ser B*, 107(2):145 – 151, 1995.
- [15] M. Mehring, D. Kotzur, and O. Kanert. Influence of the skin effect on the bloch decay in metals. *Physica Status Solidi (b)*, 53(1), 1972.
- [16] J. Tropp. Reciprocity and gyrotropism in magnetic resonance transduction. *Phys. Rev. A*, 74(6):062103, 2006.
- [17] M. V. Vaidya, C. M. Collins, D. K. Sodickson, R. Brown, G. C. Wiggins, and R. Lattanzi. Dependence of b1- and b1+ field patterns of surface coils on the electrical properties of the sample and the mr operating frequency. *Concepts Magn. Reson. B*, 46(1):25–40, 2016.
- [18] J. Van der Klink. The NMR reciprocity theorem for arbitrary probe geometry. *J. Magn. Reson.*, 148(1):147–154, 2001.